

Airborne studies of emissions from savanna fires in southern Africa

1. Aerosol emissions measured with a laser optical particle counter

P. Le Canut and M. O. Andreae

Biogeochemistry Department, Max Planck Institute for Chemistry, Mainz, Germany

G. W. Harris,¹ F. G. Wienhold, and T. Zenker

Air Chemistry Department, Max Planck Institute for Chemistry, Mainz, Germany

Abstract. During the SAFARI-92 experiment (Southern Africa Fire Atmosphere Research Initiative, September-October 1992), we flew an instrumented DC-3 aircraft through plumes from fires in various southern African savanna ecosystems. Some fires had been managed purposely for scientific study (e.g., those in Kruger National Park, South Africa), while the others were "fires of opportunity" which are abundant during the burning season in southern Africa. We obtained the aerosol (0.1-3.0 μm diameter) number and mass emission ratios relative to carbon monoxide and carbon dioxide from 21 individual fires. The average particle number emission ratio $\Delta\text{N}/\Delta\text{CO}$ (Δ : concentrations in plume minus background concentrations) varied between $14 \pm 2 \text{ cm}^{-3} \text{ ppb}^{-1}$ for grasslands and $23 \pm 7 \text{ cm}^{-3} \text{ ppb}^{-1}$ for savannas. An exceptionally high value of $43 \pm 4 \text{ cm}^{-3} \text{ ppb}^{-1}$ was measured for a sugarcane fire. Similarly, the mass emission ratio $\Delta\text{M}/\Delta\text{CO}$ varied from $36 \pm 6 \text{ ng m}^{-3} \text{ ppb}^{-1}$ to $83 \pm 45 \text{ ng m}^{-3} \text{ ppb}^{-1}$, respectively, with again an exceptionally high value of $124 \pm 14 \text{ ng m}^{-3} \text{ ppb}^{-1}$ for the sugarcane fire. The number and mass emission ratios relative to CO depended strongly upon the fire intensity. Whereas the emission ratios varied greatly from one fire to the other, the aerosol number and volume distributions as a function of particle size were very consistent. The average background aerosol size distribution was characterized by three mass modes (0.2-0.4 μm , $\approx 1.0 \mu\text{m}$, and $\approx 2.0 \mu\text{m}$ diameter). On the other hand, the aerosol size distribution in the smoke plumes showed only two mass modes, one centered in the interval 0.2-0.3 μm and the other above 2 μm diameter. From our mean emission factor ($4 \pm 1 \text{ g kg}^{-1} \text{ dm}$) we estimate that savanna fires release some 11-18 Tg aerosol particles in the size range 0.1-3.0 μm annually, a somewhat lower amount than emitted from tropical forest fires. Worldwide, savanna fires emit some $3-8 \times 10^{27}$ particles (in the same size range) annually, which is expected to make a substantial contribution to the cloud condensation nuclei population in the tropics.

Introduction

Every year, savannas in southern Africa are extensively burned in connection with agricultural and pest control practices, religious traditions, and lightning strikes [Crutzen and Andreae, 1990; Cahoon *et al.*, 1992; Andreae, 1993a]. Fires in savanna ecosystems, especially prevalent on the African continent, account for about half of the total biomass burned world-

wide [Andreae, 1993a]. Much of this burning occurs during the dry season, which in southern Africa corresponds to the period from June to September [Andreae, 1993b; Scholes *et al.*, this issue]. This large amount of burning in a limited region and in a particular season has important radiative and chemical effects on the atmosphere and influences climate on regional and global scales. Regionally, atmospheric visibility becomes very low in the dry season owing to the presence of haze and extended layers of old smoke from savanna fires [Le Canut *et al.*, 1996]. Smoke-laden air masses can be carried over long distances [Andreae *et al.*, 1994a; Garstang *et al.*, this issue; Swap *et al.*, this issue] since fine particles resulting from fires (0.1-1.0 μm diameter) are removed only slowly because of their low deposition velocity. Aerosols have a significant but complex impact on the radiative budget of the Earth [Charlson *et al.*, 1992; Andreae, 1995]. Small particles

¹Now at Centre for Atmospheric Chemistry, York University, North York, Ontario, Canada.

efficiently scatter incoming shortwave radiation and affect cloud microphysics [Charlson *et al.*, 1992; Dickinson, 1993; Andreae, 1995]. This results in a cooling of the atmosphere, which may partially compensate the warming due to the greenhouse effect [Jones *et al.*, 1994; Andreae, 1995]. However, these effects on climate are not uniform because the resulting climate forcing is spatially and temporally localized. Moreover, quantitative estimates of the cooling effect due to savanna burning are still uncertain owing to the scarcity of aerosol emission ratio values for the different types of African savanna ecosystems and owing to the wide scatter in existing data.

Aerosol emission ratios have been estimated previously for tropical savanna fires in Brazil [Ward *et al.*, 1992], for temperate ecosystems in North America [Radke *et al.*, 1991], and for aged haze layers over the equatorial and tropical South Atlantic [Andreae *et al.*, 1994a]. In 1991, the experiment FOS/DECAFE-91 (Fire of Savannas/Dynamique et Chimie Atmosphérique en Forêt Équatoriale) took place in West Africa. It was the first multidisciplinary experiment conducted in Africa to measure the gas and aerosol emissions from prescribed savanna fires [Lacaux *et al.*, 1995, Helas *et al.*, 1995]. As a result, the emission characteristics from humid savannas in Ivory Coast have been studied carefully, but information was still absent for emissions from the fires in the dry savannas of southern Africa. Consequently, the determination of aerosol emission ratios and of the size distributions of pyrogenic aerosols from savanna fires in southern Africa was one of the goals of the international measurement campaign SAFARI-92 (Southern Africa Fire Atmosphere Research Initiative), a subcomponent of the IGAC/BIBEX (International Global Atmospheric Chemistry Program/Biomass Burning Experiment) project STARE (Southern Tropical Atlantic Region Experiment) [Andreae *et al.*, 1994b]. During the 1992 dry season (September and October), measurements of trace gases and aerosol concentrations were made on board an instrumented DC-3 by a team from the Max Planck Institute for Chemistry, Mainz (Germany) (G. W. Harris *et al.*, manuscript in preparation, 1995).

In this paper, we present data on aerosol particle numbers and mass emission ratios with CO and CO₂ as reference species. We also discuss the number and volume size distributions of the smoke particles resulting from the fires encountered during SAFARI-92. The chemical composition of the pyrogenic aerosols and the emission of trace gases are discussed in companion papers (M. O. Andreae *et al.*, manuscript in preparation, 1995; G. W. Harris *et al.*, manuscript in preparation, 1995).

Methods

Measurement Techniques

The particle counter used on board the aircraft was a passive cavity aerosol spectrometer probe (model PCASP 100X; Particle Measuring Systems Inc. (PMS), Boulder, Colorado). This probe classifies particles as a function of their size into 15 bins in the range 0.10–3.0 μm diameter. The aerosol concentration was recorded every 2 s when flying through smoke plumes, and every 10 s when carrying out measurements of the regional atmospheric composition. The measurements were made at ambient humidity, which was usually low enough not to have a significant influence on particle diameters [Le Canut

et al., 1996]. Flight profiles were either stair-like transects with long horizontal legs, or spiral climbs and descents for sounding purposes.

The CO instrument was a tunable diode laser spectrometer (TDLS) using two-tone frequency modulation [Wienhold *et al.*, 1993], recording data on a 1-s time base. The CO₂ instrument was a nondispersive infrared gas analyzer (LI-COR Corporation, Lincoln, Nebraska) that also recorded data every second, but which operated with an internal time constant of 10 s, resulting in an unwanted smoothing of the CO₂ data (G. W. Harris *et al.*, manuscript in preparation, 1995).

The particle concentrations (N) are corrected to standard temperature and pressure (STP; T=20°C, P=1013.25 hPa), and are given as particles per cubic centimeter (cm⁻³). The aerosol emission ratios relative to CO are expressed in particles per cubic centimeter per part per billion CO (cm⁻³ ppb⁻¹) and those relative to CO₂ are expressed in terms of parts per million CO₂ (cm⁻³ ppm⁻¹). The mass emission ratios are given in nanogram per standard cubic meter per part per billion CO (ng m⁻³ ppb⁻¹). A specific gravity of 1.0 g cm⁻³ was assumed for the aerosol particles [Radke *et al.*, 1991]. Since the aerosol particles emitted from the fires consist mostly of organic matter, this specific gravity is an appropriate choice for the fresh smoke aerosol which is the subject of this paper. For the background aerosol and more mature plumes, which contain sulfates, nitrates, and mineral particles, a higher value is more suitable [Le Canut *et al.*, 1996].

Aerosol Number Emission Ratios

The absolute concentration of trace gases or aerosol particles in smoke samples has little significance, since it represents simply the varying degree of dilution of smoke with ambient air. This effect is particularly pronounced in aircraft sampling, where the transit time through the plume may be comparable to the sampling time. We therefore analyze our data in the form of emission ratios, e.g., the emission ratio for aerosol number concentration relative to CO concentration, ER_{N/CO}

$$ER_{N/CO} = \frac{\Delta N}{\Delta CO} = \frac{[N]_{Smoke} - [N]_{Ambient}}{[CO]_{Smoke} - [CO]_{Ambient}} \quad (1)$$

where CO or CO₂ are used as reference species. We use two

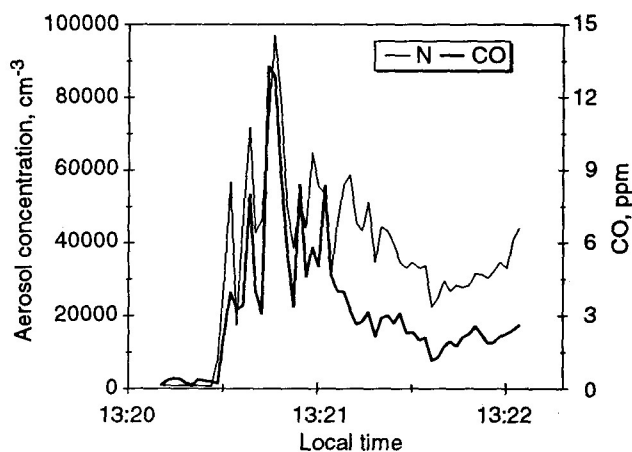


Figure 1. Carbon monoxide (CO) and aerosol concentration (N, volume corrected) time series from a pass through the smoke plume from the controlled burn on block 55 in the Pretoriuskop section of the Kruger National Park (SAF06B).

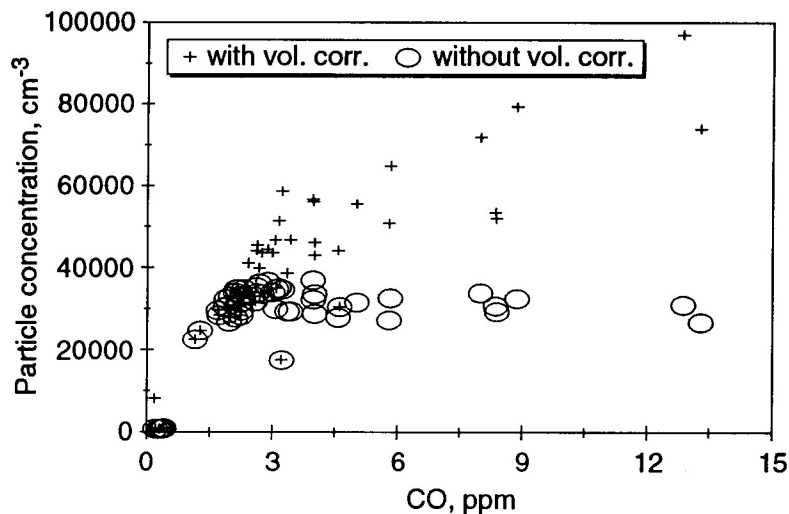


Figure 2. Aerosol particle concentration versus carbon monoxide (CO) from the same plume pass as shown in Figure 1 (crosses, volume corrected aerosol concentration; circles, aerosol concentration without volume correction).

different methods to calculate the aerosol emission ratios: the regression and the integration method. The regression method, used in most cases to obtain $\Delta N/\Delta CO$, is based on the usually very good correlation between the aerosol and carbon monoxide time series (example in Figure 1). $\Delta N/\Delta CO$ is equal to the slope (b) of the linear function $[N] = a + b \times [CO]$. However, since the PMS instrument becomes saturated when the aerosol concentration exceeds approximately $20,000 \text{ cm}^{-3}$, only the measurements from the linear part of the correlation may be used (Figure 2). At high particle concentrations, several small particles are counted as a single, apparently much bigger particle. This artifact shifts the size distribution from smaller to larger size particles and therefore also renders the sizing information unreliable. Throughout this paper, we assume that $\Delta N/\Delta CO$ in the more dilute parts of the plume typifies the entire plume.

Once we know $\Delta N/\Delta CO$, we can deduce $\Delta N/\Delta CO_2$ by

using the relation

$$\frac{\Delta N}{\Delta CO_2} = \frac{\Delta N}{\Delta CO} \times \frac{\Delta CO}{\Delta CO_2} \quad (2)$$

The associated error is $\sigma_{\Delta N/\Delta CO_2}$, which is given by the relation

$$\sigma_{\Delta N/\Delta CO_2} = \frac{\Delta N}{\Delta CO_2} \times \sqrt{\left(\frac{\sigma_{\Delta N/\Delta CO}}{\Delta N/\Delta CO}\right)^2 + \left(\frac{\sigma_{\Delta CO/\Delta CO_2}}{\Delta CO/\Delta CO_2}\right)^2} \quad (3)$$

The CO emission ratio, $\Delta CO/\Delta CO_2$, for the various fires was determined for all plume passes. This was done by integrating both the CO and the CO_2 time series for each plume pass. A direct regression calculation between CO and CO_2 was not possible because the time responses of the two instruments are different (Figure 3). $\Delta CO/\Delta CO_2$ is given by

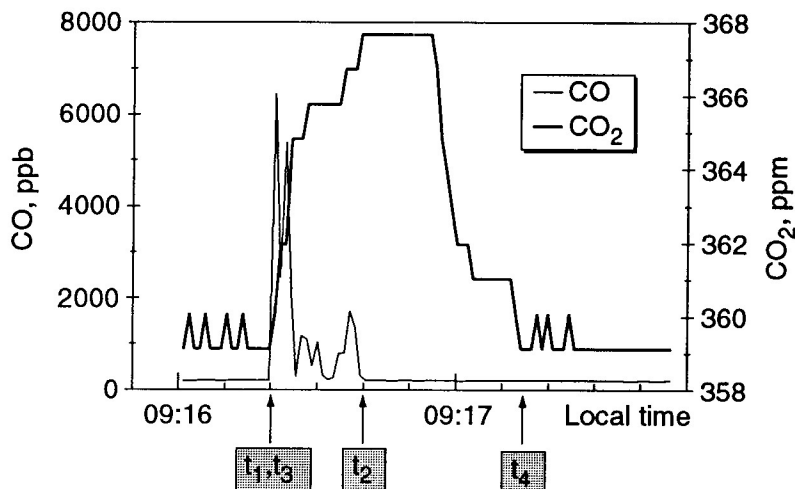


Figure 3. Carbon monoxide (CO) and carbon dioxide (CO_2) time series from a pass through the smoke plume from SAF14B. The starting times for the integration of the CO and CO_2 time series are marked by t_1 and t_3 ; the ending times are marked by t_2 and t_4 .

$$\frac{\Delta CO}{\Delta CO_2} = \frac{\int_{t_1}^{t_2} ([CO]_{Smoke} - [CO]_{Ambient}) \times dt}{\int_{t_1}^{t_2} ([CO_2]_{Smoke} - [CO_2]_{Ambient}) \times dt} \quad (4)$$

where $[CO]_{Ambient}$ and $[CO_2]_{Ambient}$ represent estimates of the background concentrations of these gases. The errors are determined by using a minimum and a maximum estimate for the background CO and CO₂ concentration levels. The minimum emission ratio $(\Delta CO/\Delta CO_2)_{Min}$ is given by

$$\left(\frac{\Delta CO}{\Delta CO_2} \right)_{Min} = \frac{\int_{t_1}^{t_2} ([CO]_{Smoke} - [CO]_{Max}) \times dt}{\int_{t_1}^{t_2} ([CO_2]_{Smoke} - [CO_2]_{Min}) \times dt} \quad (5)$$

whereas the maximum emission ratio $(\Delta CO/\Delta CO_2)_{Max}$ is obtained by inverting the indices. The error is then obtained by subtracting the minimum value from the maximum and by dividing by 2.

In a few cases, $\Delta N/\Delta CO$ could not be calculated using the regression method owing to lack of CO data. In these cases, we obtained $\Delta N/\Delta CO_2$ directly, using the same integration method as for $\Delta CO/\Delta CO_2$ (equation (4)) and estimated the error by a relationship similar to equation (5). Here also, the integration is carried out over different time intervals for N and CO₂, owing to the different time constants of the PMS and CO₂ instruments. $\Delta N/\Delta CO_2$ is therefore given by the following relation

$$\frac{\Delta N}{\Delta CO_2} = \frac{\int_{t_1}^{t_2} ([N]_{Smoke} - [N]_{Ambient}) \times dt}{\int_{t_3}^{t_4} ([CO_2]_{Smoke} - [CO_2]_{Ambient}) \times dt} \quad (6)$$

however, owing to the saturation problem of the PMS instrument, the particle concentration has to be corrected before integration. The correction used is based on the following assumptions: (1) the total volume of the corrected

particle concentration is equal to that of the uncorrected concentration and (2) the total volume is a linear function of the actual particle concentration, i.e., the shape of the distribution is constant throughout the plume. The total volume (V) is obtained by calculating the partial volumes in each channel (using the partial concentration and the average radius of each bin) and then adding up the partial volumes. Then, the function $[N] = c + d \times V$ is plotted (Figure 4). The same kind of saturation as for $[N] = a + b \times [CO]$ is seen. The slope (d) of the linear part of the curve provides the ratio $\Delta N/\Delta V$. Since the size distribution is assumed to be the same in the center as at the edge of the plume, the corrected particle concentration is given by

$$N_{corrected} = V \times \frac{\Delta N}{\Delta V} \quad (7)$$

Figure 2 shows a plot of $N_{corrected}$ versus CO and shows that the saturation almost disappears. The corrected particle concentration can consequently be integrated without great error. Nevertheless, the ratios obtained by this method must be considered lower limits of $\Delta N/\Delta CO_2$ and the method was only used for the case of the sugarcane fires sampled on flight SAF04 (Table 1), when the CO instrument performed unsatisfactorily.

Aerosol Mass Emission Ratios

Three methods are available to calculate the mass emission ratios of the smoke in the different plumes encountered. They are the regression, the integration and the average particle mass methods. The regression method is similar to that used for the aerosol number emission ratio. The same assumption applies, i.e., that $\Delta M/\Delta CO$ in the dilute parts of the plume is equal to $\Delta M/\Delta CO$ in the entire plume. Aerosol mass is obtained by multiplying the total volume (at time t) by the aerosol density, which is about 1 g cm^{-3} [Radke *et al.*, 1991]. The slope of the linear part of the function $M = a + b \times [CO]$ provides $\Delta M/\Delta CO$. Generally, the correlation coefficients for the linear regressions of number and mass are similar. This first method provides good results (high correlation coefficient) when the plume transit is relatively long.

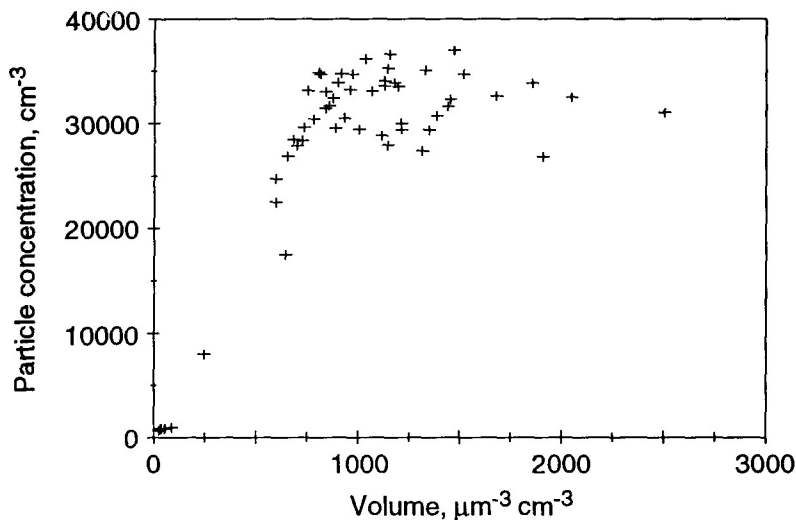


Figure 4. Particle concentration versus total aerosol volume determined from the corresponding size distribution (flight SAF06B, pass 14).

Table 1. Location, Vegetation Type, Sampling Dates and Times, and Instrument Time Base for Fire Plumes Studied During SAFARI-92

Fire Code Number	Sampling Region	Vegetation Type	Date	Local Time	Time Base
SAF04A	Big Bend, Swaziland	sugarcane	19 Sep 92	0900 - 0924	2s
SAF04B	Big Bend, Swaziland	sugarcane	19 Sep 92	0940 - 1004	2 s
SAF06A	Kruger Park, block 55, 1-13	savanna	24 Sep 92	1230 - 1320	2 s
SAF06B	Kruger Park, block 55, 14-22	savanna	24 Sep 92	1320 - 1400	2 s
SAF08B0	Zambezi River lowlands, Zambia	shrubs and grass	25 Sep 92	1412 - 1414	10 s
SAF08B00	Zambezi River lowlands, Zambia	shrubs and grass	25 Sep 92	1421 - 1423	10 s
SAF08B1	Zambezi River lowlands, Zambia	dambo	25 Sep 92	1449 - 1451	10 s
SAF08B2	Zambezi River lowlands, Zambia	dambo	25 Sep 92	1454 - 1456	10 s
SAF08B4,6,7,8	Zambezi River lowlands, Zambia	shrubs and grass	25 Sep 92	1500 - 1600	10 s
SAF08B9	Zambezi River lowlands, Zambia	shrubs and grass	25 Sep 92	1600 - 1606	10 s
SAF09A	Botswana/Namibia border	mopane forest	26 Sep 92	1156 - 1206	10, 2 s
SAF12D	plains south of Kariba	open savanna (dry)	01 Oct 92	1247 - 1250	10 s
SAF12E	mountains, 80 km ESE of Lusaka	open savanna	01 Oct 92	1316 - 1322	10 s
SAF14A	central Zambia	riparian grassland (green)	02 Oct 92	0905 - 0911	2 s
SAF14B	central Zambia	riparian grassland (dry)	02 Oct 92	0915 - 0921	2 s
SAF14C	central Zambia	open savanna (dry)	02 Oct 92	0931 - 0946	2 s
SAF14D	mountains, 80 km ESE of Lusaka	open savanna	02 Oct 92	0750 - 0753	10 s
SAF14E	NE of Lusaka, Zambia	dry grass, shrubs	02 Oct 92	0806 - 0807	10 s
SAF15A	Chobe area, Botswana	dry grass	03 Oct 92	1026 - 1031	2 s
SAF15B	western Zambia	shrubs and grass	03 Oct 92	1056 - 1102	2 s
SAF15C	western Zambia	shrubs and grass	03 Oct 92	1102 - 1107	2 s
SAF15D	Rio Cuando lowlands, Angola	grass	03 Oct 92	1120 - 1122	2 s
SAF15E	Rio Cuando lowlands, Angola	savanna	03 Oct 92	1122 - 1125	2 s
SAF15F	Rio Cuando lowlands, Angola	savanna	03 Oct 92	1125 - 1127	2 s
SAF15G	Chobe area, Botswana	dry grass	03 Oct 92	0912 - 0914	10 s

The integration method (usually applied for short transits) is similar to that used for the aerosol number emission ratio. Once the aerosol mass time series is obtained, it is integrated over the same time interval as the CO time series. Therefore $\Delta M/\Delta CO$ is given by

$$\frac{\Delta M}{\Delta CO} = \frac{\int_{t_1}^{t_2} ([M]_{Smoke} - [M]_{Ambient}) \times dt}{\int_{t_1}^{t_2} ([CO]_{Smoke} - [CO]_{Ambient}) \times dt} \quad (8)$$

The error is obtained with the method used for $\Delta CO/\Delta CO_2$ (equation (5)).

The third method is based on the average mass of a particle in pure smoke. First, the absolute size distribution of the pure smoke particles is obtained by subtracting the absolute size distribution of the background from the absolute size distribution of the plume. Then, the resulting absolute size distribution is normalized to obtain the size spectrum of the smoke particles independent of the degree of dilution with ambient air (for details on the normalization see the following section). The average mass (m) of a smoke particle is then equal to the average volume of the smoke particles times their density, where the average volume of the smoke particles is the sum of the partial volumes for a normalized size distribution of pure smoke. Finally, we apply the following relation

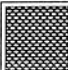
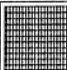
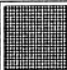

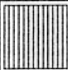
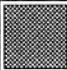



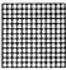
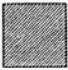
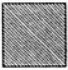


$$\frac{\Delta M}{\Delta CO} = m \times \frac{\Delta N}{\Delta CO} \quad (9)$$

The associated error is $\sigma_{\Delta M/\Delta CO}$, which is given by the relation

$$\sigma_{\Delta M/\Delta CO} = \frac{\Delta M}{\Delta CO} \times \sqrt{\left(\frac{\sigma_m}{m}\right)^2 + \left(\frac{\sigma_{\Delta N/\Delta CO}}{\Delta N/\Delta CO}\right)^2} \quad (10)$$

where σ_m is calculated from the variability of the particle mass (volume) measurements obtained during a given plume pass.

Using data from some of the longer plume transits, we calculated mass emission ratios both with the regression and with the average particle mass method to check the validity of the latter technique. The difference between the results of the two methods ranges from nil (SAF09A) to 60% (SAF06B and SAF15E) with an average of 18%. The two highest deviations can be accounted for by a high relative humidity in the cloud cap (SAF06B) and by a low correlation coefficient (0.53) for SAF15E. Without these two abnormally high values, the average difference drops to 13%, which is an acceptable agreement. Thus the average particle mass method provides a reasonable alternative to the other techniques, as long as the average size distribution does not change significantly as a function of the absolute aerosol concentration. It is not biased by the saturation artifact of the PMS probe, because the saturated particle counts and their corresponding size distributions can be discarded without invalidating the final result (mass emission ratio). This method was used when the integration method could not be applied because of saturation effects, e.g., for short transits through plumes with highly concentrated smoke.

Forests and thickets	Evergreen	
	Dry/deciduous	
Plantations	Pine/Eucalyptus	
Forest/savanna mosaic		
Woodlands, savannas and wooded grasslands	Moist/Infertile	
	Arid/Fertile	
Arid shrublands	Non-succulent	
	Succulent	
Deserts		
Sclerophyllous thickets (Fynbos)		
Grasslands	Infertile	
	Fertile	
	Grass, sedge & reed	
Wetlands and swamps	Open water	

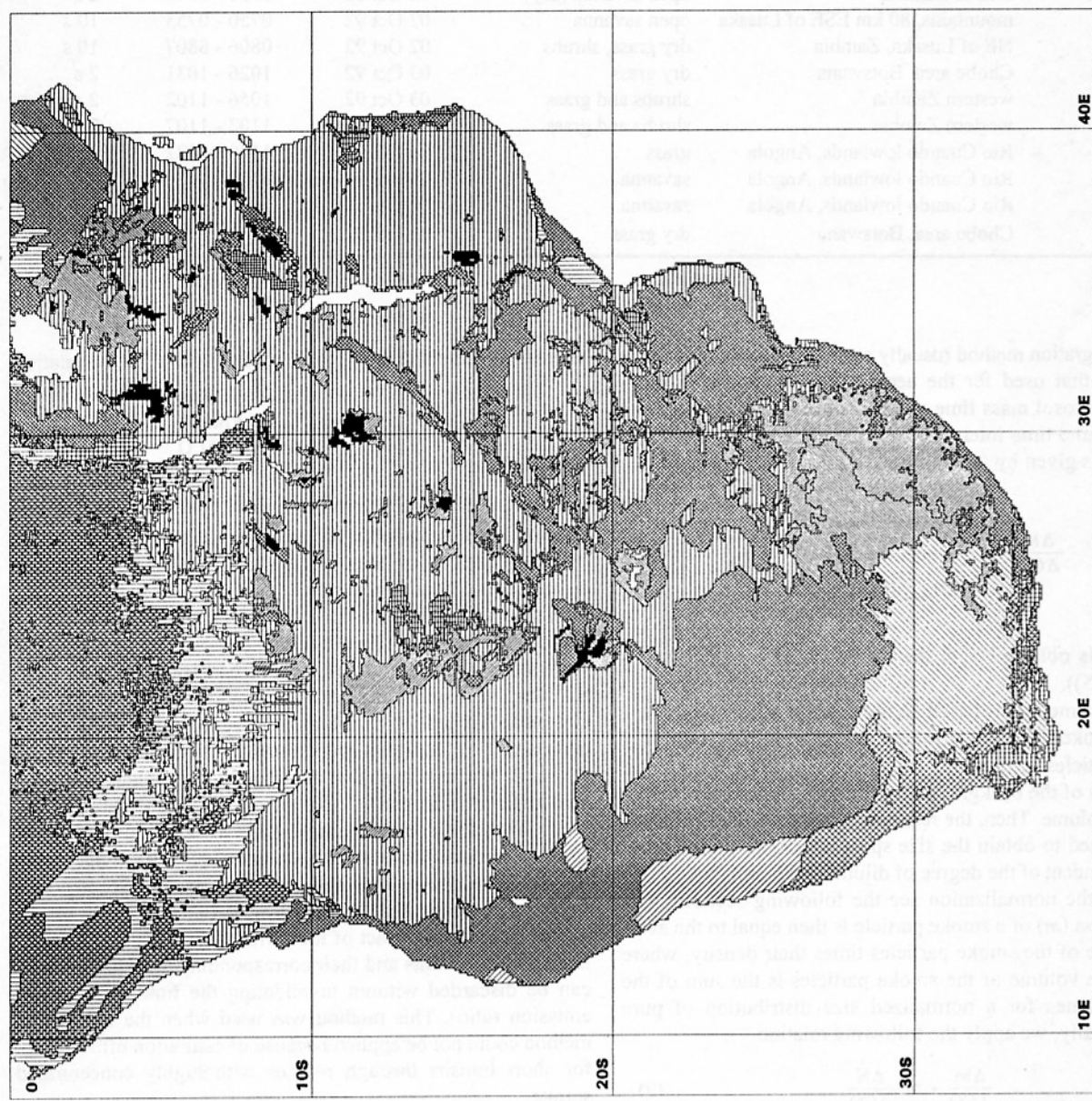


Figure 5. Location of the fires listed in Table 1 on a vegetation base map of southern Africa (modified from the vegetation fire regime map prepared by the Division of Forest Science and Technology, Council for Scientific and Industrial Research, South Africa).

Table 2. Emission Ratios, $\Delta N/\Delta CO$, $\Delta CO/\Delta CO_2$, $\Delta N/\Delta CO_2$, and $\Delta M/\Delta CO$ Measured in Smoke Plumes During SAFARI-92

Fire (Pass Number)	$\Delta N/\Delta CO$, $cm^{-3} ppb^{-1}$	r^2	$\Delta CO/\Delta CO_2$	$\Delta N/\Delta CO_2$, $cm^{-3} ppm^{-1}$	$\Delta M/\Delta CO$, $ng m^{-3} ppb^{-1}$	r^2
SAF04A (8)	43±4	0.71	0.030±0.010	1300±350	124±14	0.64
SAF04B (11)	≈30±3	...	0.030±0.010	1000±270
SAF08B0	14.5*±6	41*±37	...
SAF08B00	13*±0.8	...	0.067±0.017	870±225	31*±7	...
SAF08B1	38*±7	...	0.053±0.019	2000±800	215*±50	...
SAF08B2	39*±7	...	0.053±0.019	2100±800	168*±19	...
SAF08B9	18.3*±5	44*±17	...
SAF09A	15±0.4	0.67	0.059±0.015	885±220	45±1.6	0.63
SAF12D	40*±15	...	0.035±0.009	1400±630	185†±79	...
SAF12E	15*±12	120†±99	...
SAF14A	24±1.0	0.85	0.067±0.017	1600±400	112±7.0	0.72
SAF14B (1)	9.7±1.3	0.69	0.086±0.021	830±240	25±3.4	0.68
SAF14B (2)	10.8±1.3	0.72	0.086±0.021	930±260	29±4.0	0.65
SAF14B (3)	9.9±0.3	0.96	0.08±0.02	790±200	22±1.0	0.93
SAF14C (2)	10.8±0.6	0.86	0.06±0.015	650±170	38±1.5	0.92
SAF14C (3)	22±1.6	0.74	0.054±0.013	1200±310	52±6.4	0.5
SAF14C (4)	20±1.0	0.88	0.08±0.02	1600±410	57±6.1	0.85
SAF14D	16*±6	...	0.032±0.008	510±230	80†±34	...
SAF14E	28*±2	...	0.052±0.013	1450±380	106†±23	...
SAF15A (1)	11.5±0.8	0.72	0.049±0.012	560±145	34±3.0	0.63
SAF15A (2)	9.9±0.2	0.95	0.067±0.017	660±165	26±1.0	0.88
SAF15B (1)	16.5±0.9	0.85	40±6.1	0.43
SAF15B (2)	14.1±1.0	0.77	0.069±0.017	970±250	38±6.4	0.4
SAF15B (3)	19.8±0.8	0.91	0.053±0.013	1050±265	45±3.9	0.7
SAF15C (1)	15.3±0.3	0.94	0.071±0.018	1090±275	45±3.3	0.6
SAF15C (2)	14.5±1.3	0.95	0.038±0.009	550±140	33†±7	...
SAF15D	15.1±1.4	0.9	0.067±0.017	1010±270	33±7.6	0.26
SAF15E	30.4±3.7	0.94	0.026±0.06	790±220	28±2.9	0.53
SAF15F	21.1±2.8	0.74	0.065±0.016	1370±380	49†±12	...
SAF15G	19*±2	...	0.047±0.011	940±255	70†±16	...

* Integration method, † Average particle mass method.

Size Distributions

Size distributions were obtained for most fire plumes and for the background aerosol in the region adjacent to the plumes. The PMS instrument provides size distribution data in terms of particle number concentrations in each size bin. To compare the size distributions resulting from the various fires between each other and with the background aerosol, they are normalized by dividing the concentration in each bin by the total concentration, i.e., the sum of the values in all the bins. The normalized size distribution is therefore independent of the absolute concentration, which depends on dilution, as discussed above. The results are shown as plots of $dN/d\log(d)$ versus $\log(d)$, since using the logarithmic derivative makes the distribution appear less steep and shows more detail in the coarse size range. The same type of representation ($dV/d\log(d)$ versus $\log(d)$) was used for the volume distributions, where V stands for the normalized volume concentration, i.e., the volume in each size bin divided by the total volume.

Results and Discussion

During SAFARI-92, the instrumented DC-3 flew through the smoke plumes of several controlled fires and numerous "fires of opportunity". The plume passes were flown by enter-

ing the fire plume from the upwind side and climbing up in the plume as close as possible to its central axis. Each individual fire was assigned a code based on the flight number. A list of these fires with their sampling date and time, and the type of biomass burned are given in Table 1. The location of the fires is shown on a map of southern Africa (Figure 5). We calculated the following emission ratios for each pass through the plume of these fires: the CO-to-CO₂ emission ratio ($\Delta CO/\Delta CO_2$) as an indicator of combustion conditions and to convert CO-based to CO₂-based emission ratios, the particle number emission ratios $\Delta N/\Delta CO$ and $\Delta N/\Delta CO_2$, and the particle mass emission ratios $\Delta M/\Delta CO$ and $\Delta M/\Delta CO_2$. The results are presented in the following paragraphs.

CO Emission Ratios ($\Delta CO/\Delta CO_2$)

The emission of CO from the fires investigated during SAFARI-92 is discussed in detail in several other papers [Andreae et al., 1996; Koppmann et al., 1996; Cofer et al., this issue; Lacaux et al., this issue; Ward et al., this issue; G. W. Harris et al., manuscript in preparation, 1995; G. Helas et al., manuscript in preparation, 1995]. The observed CO emission ratios typically fall in the range 0.03-0.08, with an average of 0.057 (Table 2). The average error in the determination of the CO emission ratio is 25%, based on the use of equation (5).

Table 3. Aerosol Particle Number and Mass Emission Ratios for the Smoke Plume From the Fire on Kruger National Park Block 55 (SAF06)

Plume Pass Number	$\Delta N/\Delta CO_2$, $cm^{-3} ppb^{-1}$	r^2	$\Delta M/\Delta CO_2$, $ng m^{-3} ppb^{-1}$	r^2
1	22.2±1.3	0.88	60.2±3.4	0.89
2	17.6±1.3	0.82	60.6±3.9	0.86
3	25.4±1.7	0.87	82.2±6.6	0.86
4	25.2±2.0	0.79	76.6±5.3	0.83
5	24.7±1.3	0.85	68.5±3.7	0.85
6	23.6±1.6	0.78	80.8±5.3	0.8
7	43.1±1.4	0.93	133.5±6.0	0.88
8	35.0±3.3	0.68	103.6±8.6	0.74
9	24.5±1.0	0.88	76.6±2.9	0.89
10	26.9±1.1	0.89	74.3±3.3	0.88
11	36.2±2.2	0.79	103.8±6.8	0.77
12	25.1±2.3	0.69	64.1±6.4	0.66
13	52.2±4.1	0.78	138.9±12.6	0.75
Average, SAF06A (1-13)	29.4±9.6	0.82±0.08	86±26	0.82±0.07
14	18.8±0.9	0.93	66.5±2.8	0.94
15	7.4±1.6	0.38	41.1±8.6	0.38
16	13.9±0.7	0.87	43.8±7.6	0.83
17	9.5±0.6	0.91	53.1±6.1	0.76
18	10.3±0.7	0.85	39.3±3.4	0.79
19	14.0±1.3	0.92	55.2±6.8	0.87
20	21.6±0.7	0.93	78.7±4.7	0.81
21	17.4±0.9	0.83	69.8±3.8	0.82
22	14.6±0.6	0.85	70.4±3.3	0.88
Average, SAF06B (14-22)	14.2±4.6	0.83±0.17	57.5±14.4	0.78±0.17
Overall average	23.1±10.9	0.82±0.12	74.6±26.0	0.80±0.12

This average error is used in Table 2 to estimate the errors of all the CO-to-CO₂ emission ratios. The lowest $\Delta CO/\Delta CO_2$ values were measured in some intensive, flaming fires (e.g., the sugarcane burns of SAF04), while the highest values were observed over moist grasslands (e.g., SAF14A and SAF14B). Considerably higher CO emission ratios (up to 0.11) were measured during SAFARI-92 from subtropical forest fires [Andreae *et al.*, 1996], but since we did not obtain particle emission data from these fires, they are not discussed here. This emission behavior agrees with that previously reported for similar environments [e.g., Ward *et al.*, 1992; Lacaux *et al.*, 1995] (see also the companion papers cited above).

Particle Number Emission Ratios

Table 2 shows the particle emission ratios for all transits through fire plumes, with the exception of the measurements made on the fire on block 55 in Kruger Park (Flight SAF06), which are given in Table 3. Details on the results from the various flights are presented below.

Flight SAF04. On 19 September 1992, the DC-3 flew over two sugarcane fires on the Ubombo Ranches plantation near Big Bend, Swaziland. There were eight passes through the plume from each fire. These passes are numbered 1 to 8 for the first fire and 9 to 16 for the second. Although CO mixing ratios are available for passes 4 to 14, instrument problems resulted in poor data quality, and a regression fit between the CO and aerosol time series was not possible for most of the

passes. For the first fire (SAF04A), on the smaller sugarcane field (12 ha), only pass 8 provides a reasonable fit ($r^2 = 0.71$). For the second fire (SAF04B), which was conducted on a larger plot (43.7 ha) and which had a very intensive flame development, only pass 11 could be used. The regression method yields a $\Delta N/\Delta CO_2$ emission ratio of $43 \pm 4 \text{ cm}^{-3} \text{ ppb}^{-1}$ for SAF04A, and the one for SAF04B can be estimated at $30 \pm 3 \text{ cm}^{-3} \text{ ppb}^{-1}$. Since the $\Delta CO/\Delta CO_2$ emission ratios for passes 8 and 11 are both equal to 0.03 ± 0.01 , $\Delta N/\Delta CO_2$ is $1300 \pm 350 \text{ cm}^{-3} \text{ ppm}^{-1}$ for SAF04A and $1000 \pm 270 \text{ cm}^{-3} \text{ ppm}^{-1}$ for SAF04B. To double-check these values, we also investigated the $\Delta N/\Delta CO_2$ emission ratios for these two fires using the integration method. We obtained $\Delta N/\Delta CO_2 = 1420 \pm 350 \text{ cm}^{-3} \text{ ppm}^{-1}$ for pass 8 and $1460 \pm 350 \text{ cm}^{-3} \text{ ppm}^{-1}$ for pass 11. These values are very similar, as expected from two fires of the same type. For SAF04A, the integration method gives an estimate very close to the result obtained by the regression method. The match is not as good for SAF04B owing to the much greater uncertainty in the $\Delta N/\Delta CO_2$ emission ratio. Therefore we propose the $\Delta N/\Delta CO_2$ emission ratio of SAF04A ($1300 \pm 350 \text{ cm}^{-3} \text{ ppm}^{-1}$) as the best estimate for particle emission from the sugarcane fires investigated.

Flight SAF06. On 24 September 1992, a controlled burn was conducted on block 55 in the Pretoriuskop section of Kruger National Park. The fire started at 0921 LT and ended at 1458 LT. Details on fuel and fire behavior during this burn are presented by Stocks *et al.* [this issue]. Between 1235 LT and

Table 4. Emission Ratios, Combustion Efficiencies, and Emission Factors (EF) From Fires in the Various Ecosystems Studied in Southern Africa During SAFARI-92

Fire	$\Delta N/\Delta CO$,		$\Delta N/\Delta CO_2$,	$\Delta M/\Delta CO$,	$\Delta M/\Delta CO_2$,	Combustion	EF,
	$cm^{-3} ppb^{-1}$	$\Delta CO/\Delta CO_2$					
<i>Sugarcane Fields</i>							
SAF04A (peak 8)	43±4	0.030±0.010	1300±350	124±14	3.7±0.8	0.965	2.8
<i>Grasslands, Infertile and Fertile</i>							
SAF08B0	14.5*±6	41*±37
SAF08B00	13*±0.8	0.067±0.017	870±225	31*±7	2.1±0.7	0.926	1.6
SAF09A (fertile)	15±0.4	0.059±0.015	885±220	45±1.6	2.6±0.7	0.934	2
SAF14B	10±1.8	0.084±0.036	850±400	25±5	2.1±1.0	0.908	1.6
SAF15A	10±0.7	0.058±0.02	600±215	30±3.0	1.7±0.6	0.935	1.3
SAF15B	16.8±1.6	0.061±0.021	1010±365	41±10	2.5±1.0	0.932	1.9
SAF15C	14.9±1.4	0.054±0.019	820±290	39±9	2.1±0.9	0.939	1.6
SAF15D	15.1±1.4	0.067±0.017	1010±270	33±7.6	2.2±0.8	0.926	1.7
Average	14±2.3	0.064±0.009	860±130	36±6.5	2.2±0.3	0.94±0.23	1.7±0.2
<i>Dambos</i>							
SAF08B1	38*±7	0.053±0.019	2000±800	215*±50	11±5	0.944	8.3
SAF08B2	39*±7	0.053±0.019	2100±800	168*±19	8.9±3.6	0.944	6.8
Average	38	0.053±0.019	2000±800	190±50	9.9±5.7	0.944	7.6±0.8
<i>Savannas, Fertile and Infertile</i>							
SAF06	23±11	0.051±0.023	1170±560	75±26	3.8±1.3	0.944	2.9
SAF08B9	18*±5	44*±17
SAF12D (fertile)	40*±15	0.035±0.009	1400±630	185†±79	6.5±3.2	0.960	4.9
SAF12E	15*±12	120†±99
SAF14A	24±1.0	0.067±0.017	1600±400	112±7.0	7.5±1.9	0.926	5.7
SAF14C	18±1.8	0.064±0.027	1150±515	49±8	3.1±1.4	0.928	2.4
SAF14D	16*±6	0.032±0.008	510±230	80†±34	2.6±1.3	0.963	1.9
SAF14E	28*±2	0.052±0.013	1450±380	106†±23	5.5±1.8	0.941	4.2
SAF15E	30±4	0.026±0.006	790±220	28±2.9	0.7±0.2	0.970	2.1
SAF15F	21±3	0.065±0.016	1370±380	49†±12	3.2±1.1	0.928	2.4
SAF15G	19*±2	0.047±0.011	940±255	70†±16	3.3±1.1	0.947	2.5
Average	23±7	0.048±0.025	1150±350	83±45	4.0±2.1	0.95±0.02	3.2±1.4

* Integration method, † Average particle mass method.

1400 LT, the DC-3 flew 22 passes through the smoke plume. On all the passes, the PMS probe became saturated in the center of the plume owing to the thickness of the smoke, so that only data from the outer parts of the plume could be used. For each pass, $\Delta N/\Delta CO$ has been calculated (Table 3), as well as the correlation coefficient of the linear regression (r^2). Most of the r^2 values are between 0.8 and 0.9, indicating reliable estimates of the regression slope.

The 22 passes can be partitioned into two sets that show distinct characteristics, with the differences in sampling altitude and in plume age probably accounting for the difference between the two sets. The first 13 passes were flown at an altitude of approximately 1500 m above mean sea level (amsl; approximately 1000 m above ground level (agl)), whereas passes 14 to 22 were higher, in the developing cloud cap, at approximately 2500 m amsl (~ 2000 m agl). These sampling heights correspond to the approximate rise height of the plume at the time of sampling. The average particle number emission ratio for the first 13 passages is $29 \pm 10 cm^{-3} ppb^{-1}$, compared to $14 \pm 5 cm^{-3} ppb^{-1}$ for the last nine passes. The lower values at higher altitudes and in the cloud cap may be the result of coagulation processes in the plume. Koppmann *et al.* [1996] found a mean CO emission ratio for SAF06 of 0.051 ± 0.023 ,

which corresponds to mean $\Delta N/\Delta CO_2 = 1170 \pm 560 cm^{-3} ppm^{-1}$ for this fire (Table 4).

Flight SAF08B. On 25 September 1992, a fire survey flight was conducted over western Zambia, between Victoria Falls and Zambezi. The instrumented DC-3 flew through the plumes of nine savanna fires. These fires were quite small, with fire lines extending typically over only a few hundred meters. They were burning in grassy and shrubby vegetation in the lowlands of the Zambezi River. Their proximity to native settlements suggests that they had been set in connection with native land use practices. This type of fire was the one most frequently observed during the SAFARI-92 flights, and, based on our in-flight observations and on remote-sensing information, hundreds of such fires were active in the region. Many of these fires were burning as backfires, i.e., against the wind direction, presumably as a result of native fire management practices. Such fires produce relatively clean burns, with highly effective combustion and correspondingly low CO and aerosol emission ratios (e.g., SAF08B-0, SAF08B-00, and SAF08B-9 in Table 2).

During flight SAF08, we also flew through the plumes of two fires (SAF08B-1 and SAF08B-2) burning in seasonally flooded grasslands (dambos). They showed significantly

higher aerosol emission ratios than the other savanna fires encountered during this and the following survey flights, with the exception of the fire in the fertile savanna at SAF12D (Table 2). At the time of our flight, most of the dambos had already been burned over, as evident from black fire scars. For four fires (SAF08B-4, SAF08B-6, SAF08B-7, and SAF08B-8), aerosol emission ratios could not be obtained because of instrument limitations.

Flight SAF09A. On 26 September 1992, on the way from Victoria Falls (Zimbabwe) to Maun (Botswana), the DC-3 flew through a plume (SAF09A) from a very large savanna fire in a mopane forest north of Okavango, near the Botswana-Namibia border. The aircraft flew along the fire front for over 10 min. This fire was burning as a backfire along much of the fire front, and the measured aerosol emission ratio was $15 \pm 0.4 \text{ cm}^{-3} \text{ ppb}^{-1}$. Given a $\Delta\text{CO}/\Delta\text{CO}_2$ emission ratio of 0.059 ± 0.015 for this fire, the aerosol emission ratio relative to CO_2 was $885 \pm 220 \text{ cm}^{-3} \text{ ppm}^{-1}$.

Flight SAF12. During a regional survey flight on 1 October 1992 from Pretoria, South Africa, to Lusaka, Zambia, we intercepted plumes from a savanna fire in the plains south of Lake Kariba (SAF12D; $17^\circ 17' \text{S}$, $28^\circ 53' \text{E}$) and from several fires in the mountains about 80 km ESE of Lusaka (SAF12E). Since the aircraft was at high altitude and considerable distance from these fires, the fuel type could not be determined specifically. The region where the fires occurred was, however, dominated by open savanna with a dry grass stratum, and we assume that this type of material provided the fuel for these fires. The four distinguishable plumes from the mountain fires (SAF12E), which were encountered at about 1500 m agl, had particle number emission ratios ($13\text{--}17 \text{ cm}^{-3} \text{ ppb}^{-1}$) similar to those observed elsewhere in the Zambian savanna. The plume from SAF12D, on the other hand, had risen to an altitude of 3000 m agl and must have originated from an intensively burning fire. Its emission characteristics resemble the sugarcane fires (SAF04), with a $\Delta\text{N}/\Delta\text{CO}$ of $40 \pm 15 \text{ cm}^{-3} \text{ ppb}^{-1}$, a $\Delta\text{M}/\Delta\text{CO}$ of $185 \pm 79 \text{ ng m}^{-3} \text{ ppb}^{-1}$, and a $\Delta\text{CO}/\Delta\text{CO}_2$ of 0.035 ± 0.009 . The aerosol number and mass emission ratios from this fire are thus significantly greater than the values typical of the small savanna fires most common in Zambia. This may reflect a tendency toward higher emission ratios in intensively burning fires, where the heat release is great enough to result in a plume rise of several thousand meters.

Flight SAF14. On 2 October 1992, three savanna fires were investigated in detail in central Zambia (SAF14A-C; 14°S , $27\text{--}28^\circ \text{E}$). In addition, we briefly sampled smoke (SAF14D) from fires in the same mountainous area ESE of Lusaka as on SAF12, and from a small fire on a mountain ridge NE of Lusaka (SAF14E; $15^\circ 00' \text{S}$, $28^\circ 47' \text{E}$). The smoke from the mountain fires had characteristics nearly identical to those observed the previous afternoon (SAF12E; Table 2). The small mountain fire (SAF14E) was sampled close to ground level; the fuel was dry grass growing between small trees and shrubs. The somewhat elevated aerosol and CO emission ratios suggest a significant smoldering component.

In the case of SAF14A and SAF14B, the fires were in grasslands near a river. The grass fuel in SAF14A was relatively green, while the fuel in SAF14B appeared considerably drier. The fires were burning mostly as head fires. There were three passes through the plume from SAF14A, which were lumped together to obtain enough data for a reliable regression analysis. We obtained $\Delta\text{N}/\Delta\text{CO} = 24 \pm 1.0 \text{ cm}^{-3} \text{ ppb}^{-1}$, consistent with a significant smoldering component in the relatively moist fuel. $\Delta\text{CO}/\Delta\text{CO}_2$ was 0.067 ± 0.017 , giving a $\Delta\text{N}/\Delta\text{CO}_2$

of $1600 \pm 400 \text{ cm}^{-3} \text{ ppm}^{-1}$. On the other hand, the three passes through the plume resulting from SAF14B could be analyzed separately to calculate the emission ratios. As expected for the drier fuel type in this fire, the $\Delta\text{N}/\Delta\text{CO}$ for SAF14B are lower (9.7 ± 1.3 , 10.8 ± 1.3 , and $9.9 \pm 0.3 \text{ cm}^{-3} \text{ ppb}^{-1}$); the corresponding $\Delta\text{N}/\Delta\text{CO}_2$ are 830 ± 240 , 930 ± 260 , and $790 \pm 200 \text{ cm}^{-3} \text{ ppm}^{-1}$, respectively. The two ratios for all three passes are relatively constant and therefore yield a reliable average for this fire ($10 \pm 1.8 \text{ cm}^{-3} \text{ ppb}^{-1}$ and $850 \pm 400 \text{ cm}^{-3} \text{ ppm}^{-1}$, Table 4).

In contrast to many of the other fires encountered in the Zambian savanna, which burned as small backfires and produced a thin smoke plume, SAF14C was a quite intense head fire in the dry, grassy stratum of an open savanna, producing thick white to yellowish smoke. The four passes through the plume resulting from SAF14C were analyzed separately. No result could be derived from the first pass owing to the very brief transit through the plume. For the second, third and fourth passes, $\Delta\text{N}/\Delta\text{CO}$ are 10.8 ± 0.6 , 22 ± 1.6 , and $20 \pm 1.0 \text{ cm}^{-3} \text{ ppb}^{-1}$, respectively. With corresponding $\Delta\text{CO}/\Delta\text{CO}_2$ emission ratios of 0.06 ± 0.015 , 0.054 ± 0.013 , and 0.08 ± 0.02 , we evaluate $\Delta\text{N}/\Delta\text{CO}_2$ as 650 ± 170 , 1200 ± 310 , and $1600 \pm 410 \text{ cm}^{-3} \text{ ppm}^{-1}$. For this fire, the average emission ratios are thus $18 \pm 1.8 \text{ cm}^{-3} \text{ ppb}^{-1}$ and $1150 \pm 515 \text{ cm}^{-3} \text{ ppm}^{-1}$ (Table 4), consistent with a tendency for higher emissions from more intense fires.

Flight SAF15. On 3 October 1992, several savanna fires were surveyed in Botswana, Zambia, and Angola. SAF15G, in the Chobe area of Botswana, was a very small fire burning as a head fire in dry, yellow grass. The next fire, SAF15A, also had a very short front and was burning in the grassy stratum of a dry, barren-looking savanna. The average particle emission ratios measured during two passes through this fire were quite low, $10 \pm 0.7 \text{ cm}^{-3} \text{ ppb}^{-1}(\text{CO})$ and $600 \pm 215 \text{ cm}^{-3} \text{ ppm}^{-1}(\text{CO}_2)$ (Table 4), with less than 10% difference between the two passes (Table 2). The next two fires, SAF15B and SAF15C, in western Zambia, burned in dry, grassy areas which surrounded small "islands" of savanna vegetation. Both had the relatively low average emission ratios typically observed for this type of fire: $\Delta\text{N}/\Delta\text{CO}$ was 16.8 ± 1.6 and $14.9 \pm 1.4 \text{ cm}^{-3} \text{ ppb}^{-1}$, and $\Delta\text{N}/\Delta\text{CO}_2$ was 1010 ± 365 and $820 \pm 290 \text{ cm}^{-3} \text{ ppm}^{-1}$ (Table 4). The final three fires investigated during this flight were located in the lowlands of the Rio Cuando in southeastern Angola. The first of these, SAF15D, was a head fire in a grassy floodplain with greenish-yellow grass as the dominant fuel. For this type of fuel, which appeared similar to the vegetation burning in the dambos of SAF08B-1 and SAF08B-2, the observed particle emission ratio is surprisingly low, $15.1 \pm 1.4 \text{ cm}^{-3} \text{ ppb}^{-1}$. On the other hand, SAF15-E and SAF15-F were burning in the savanna, somewhat farther away from the Rio Cuando. These fires were quite intense and had large volumes of black smoke in the plumes, indicative of intensively flaming combustion. The very low $\Delta\text{CO}/\Delta\text{CO}_2$ measured in SAF15E suggests that the aircraft penetrated the emissions from the most intense part of this fire. Correspondingly, a high $\Delta\text{N}/\Delta\text{CO}$ ($30.4 \pm 3.7 \text{ cm}^{-3} \text{ ppb}^{-1}$), but only a moderate $\Delta\text{N}/\Delta\text{CO}_2$ of $790 \pm 220 \text{ cm}^{-3} \text{ ppm}^{-1}$ were measured. In SAF15F, the aircraft encountered smoke from both the flaming and the smoldering zones, resulting in a lower particle emission ratio relative to CO and a higher ratio relative to CO_2 .

Aerosol Mass Emission Ratios

The mass emission ratios ($\Delta\text{M}/\Delta\text{CO}$) for all fires are shown in Table 2. For most of the fires, the transit time was long enough to provide sufficient data points for us to use the re-

gression method to obtain emission ratios. The average uncertainty of the regression slope obtained with this method is about 10% ($N=17$), and the correlation coefficients are relatively high (Table 2). For some short plume passes, the integration method had to be used (SAF08B-0, SAF08B-00, SAF08B-1, SAF08B-2, and SAF08B-9). For this method, the average error is about 37% ($N=5$), much higher than for the regression method. Finally, in those cases where the mass emission ratios produced by the integration method were unreliable because of instrument saturation problems (SAF12D, SAF12E, SAF14D, SAF14E, SAF15C, SAF15F, and SAF15G), we used a third approach, the average particle mass method. The average error using this method is 40% ($N=6$), slightly higher than with the integration method.

The mass emission ratios measured during SAFARI-92 vary from $22 \pm 1.0 \text{ ng m}^{-3} \text{ ppb}^{-1}$ for SAF14B (third transit) to 215 ± 50 for SAF08B1. Averages for the various ecosystems studied range from $36 \pm 6.5 \text{ ng m}^{-3} \text{ ppb}^{-1}$ for the grassland fires to $83 \pm 45 \text{ ng m}^{-3} \text{ ppb}^{-1}$ for the savanna fires (Table 4). These ratios are in reasonable agreement with literature values that typically fall in the range of 40 to $180 \text{ ng m}^{-3} \text{ ppb}^{-1}$. [Andreae et al., 1988; Einfeld et al., 1991; Radke et al., 1991; Ward et al., 1991; Ward and Hardy, 1991; Scholes et al., this issue]. The lowest ratios in the literature have been reported from savanna fires: $40 \pm 14 \text{ ng m}^{-3} \text{ ppb}^{-1}$ [Andreae et al., 1994a] and $44 \pm 18 \text{ ng m}^{-3} \text{ ppb}^{-1}$ [Ward et al., 1992], and our lower ratios agree well with these figures. The highest ratios observed in our study were found over very intensive fires (sugarcane) and over fires in the dambos. Emission ratios from these fires approach the values typical of forest fires [Einfeld et al., 1991; Radke et al., 1991; Ward et al., 1991; Ward and Hardy, 1991].

Aerosol mass and number emission ratios from all SAFARI-92 fires are plotted versus the CO emission ratio in Figures 6a and 6b. In both cases, the aerosol emission ratios (relative to CO) decline with increasing $\Delta\text{CO}/\Delta\text{CO}_2$. The correlation coefficients are identical for both regressions ($r=-0.59$; $\alpha=0.005$). On the other hand, there is no detectable correlation between the aerosol emission ratios relative to CO_2 and $\Delta\text{CO}/\Delta\text{CO}_2$, which indicates that in this data set, there is no relationship between the efficiency of aerosol production and the amount of smoldering combustion. Such a relationship has been previously observed in several studies, especially when savanna and forest fires were compared [e.g., Ward et al., 1992]. The increase in emission ratios relative to CO at

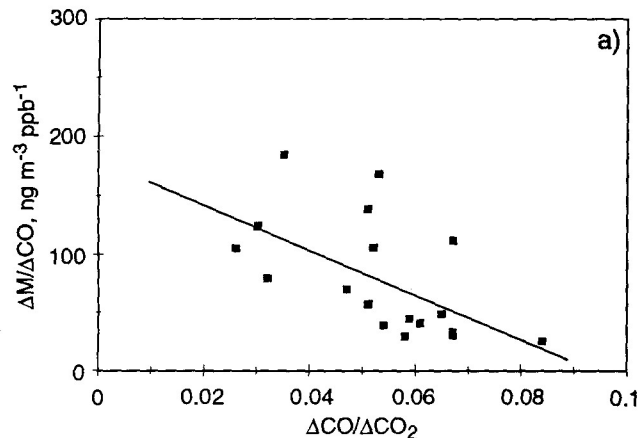


Figure 6a. Aerosol mass emission ratios ($\Delta M/\Delta\text{CO}$) plotted versus carbon monoxide emission ratios ($\Delta\text{CO}/\Delta\text{CO}_2$) for the fires listed in Table 4.

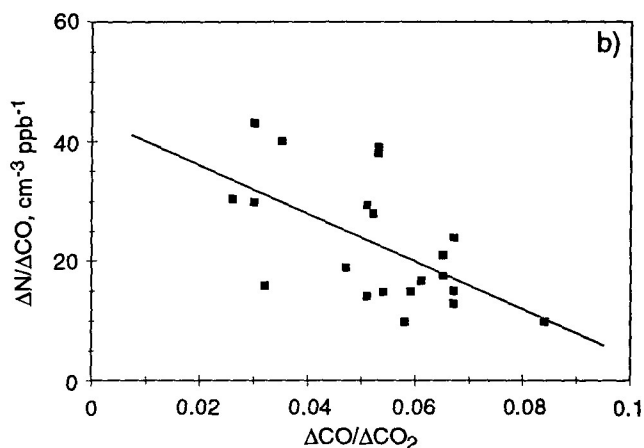


Figure 6b. Aerosol number emission ratios ($\Delta N/\Delta\text{CO}$) plotted versus carbon monoxide emission ratios ($\Delta\text{CO}/\Delta\text{CO}_2$) for the fires listed in Table 4.

low $\Delta\text{CO}/\Delta\text{CO}_2$, i.e., from intensively flaming fires such as those at SAF12D and the sugarcane fields is due to a combination of two effects: (1) low CO emissions from flaming combustion, leading to low values of ΔCO in the denominator of the emission ratios and (2) the effective production of black carbon aerosol and mobilization of mineral ash particles in these fires which results in an increase in the amount of aerosol emitted per unit of biomass burned. The highest aerosol emission ratios relative to CO_2 were measured from the two dambo fires. Unfortunately, such fires were encountered infrequently during SAFARI-92, and we do not have adequate statistics for this fire regime. However, many fire scars were evident in dambos along our flight paths, and it is likely that dambo fires produce substantial amounts of atmospheric aerosols earlier in the season.

Emission Factors

On the basis of the emission ratio data discussed above, we estimated emission factors (EF) and combustion efficiencies (CE) for all the fires studied (Table 4). The emission factor is defined as the amount of a compound released per amount of fuel consumed (grams per kilogram dm; dm: dry matter), and the combustion efficiency is defined as the fraction of carbon emitted as CO_2 relative to the total gaseous carbon emitted by the fire [Ward et al., 1992]. When detailed data on carbon species other than CO_2 and CO are lacking, CE can be estimated using the relation

$$\text{CE} = \frac{\Delta\text{CO}_2}{\Delta\text{CO}_2 + \Delta\text{CO} + \sum_i \Delta\text{gas}_i} \approx \frac{1}{1 + 1.2 \times \frac{\Delta\text{CO}}{\Delta\text{CO}_2}} \quad (11)$$

For the calculation of the emission factors, we assumed a carbon content of 45% in dry biomass [Andreae, 1993a]. Figure 7 shows a plot of the emission factors versus the combustion efficiencies for the fires studied. All of the fires have a relatively high CE (0.9 to 1.0), consistent with the results of Ward et al. [this issue], who found an average CE of 0.93 for experimental savanna fires in southern Africa. The lowest emission factors are observed for grasslands ($1.7 \pm 0.2 \text{ g kg}^{-1} \text{ dm}$), the highest for dambo fires ($7.6 \pm 0.8 \text{ g kg}^{-1} \text{ dm}$). Savanna fires have an average emission factor of $3.2 \pm 1.4 \text{ g kg}^{-1} \text{ dm}$.

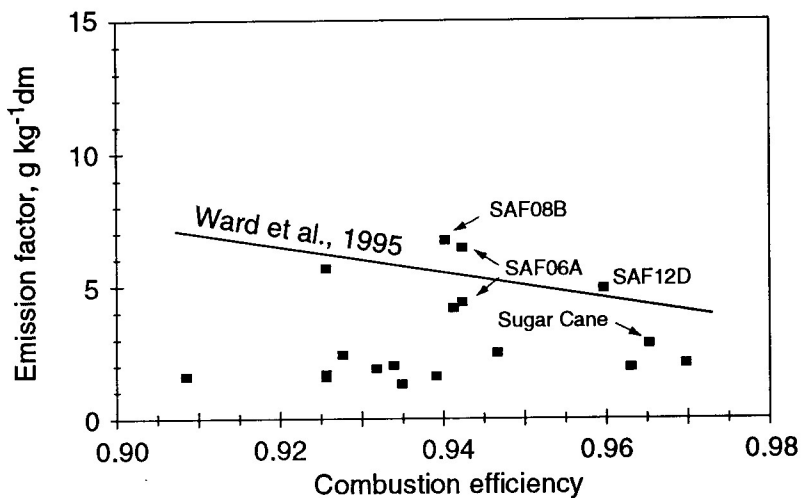


Figure 7. Emission factors (grams per kilogram dry matter) of the fires listed in Table 4 plotted against the corresponding combustion efficiencies.

The limited range of combustion efficiencies represented by our data does not allow the calculation of a useful relationship between the aerosol emission factor and CE. Our data plot reasonably close to the regression line obtained by *Ward et al.* [this issue] from ground-based measurements on experimental fires in Zambia and South Africa (Figure 7). The data from the more intense fires show the best agreement; in particular, our results from the KNP block 55 fire (SAF06-A and SAF06-B) straddle *Ward et al.*'s regression line. On the other hand, the numerous small, low-intensity fires we found in Zambia tend to fall well below the regression line, suggesting that this type of fire may not have been well represented by the experimental burns studied by *Ward et al.* [this issue].

Scholes et al. [this issue] derived regional estimates of aerosol and trace gas emissions from fires in southern Africa by multiplying the emission factor data from *Ward et al.* [this issue] with the amounts of carbon burned in the various regional ecosystems; considering fire frequency statistics for these ecosystems. They obtain a regional mean aerosol emission factor of $5.5 \text{ g kg}^{-1} \text{ dm}$. When forest fires are excluded from their data set, this estimate is reduced to $4.8 \text{ g kg}^{-1} \text{ dm}$, representing fires in savannas and grasslands. A similar weighting applied to our emission factor data would result in a value of $3.6 \text{ g kg}^{-1} \text{ dm}$. We consider this agreement reasonably good, given the difference in methodology between the two groups. *Ward et al.* [this issue] sampled from masts near the ground and may have sampled a higher proportion of the smoldering emissions than our airborne measurements. This is suggested by their average $\Delta\text{CO}/\Delta\text{CO}_2$ of 0.074, which is considerably higher than our value. This difference alone could account for most of the discrepancy in emission factors. In fact, if we estimate a regional mean $\Delta\text{M}/\Delta\text{CO}$ from our emission ratios and the CO emission statistics given by *Scholes et al.* [this issue] ($78 \text{ ng m}^{-3} \text{ ppb}^{-1}$) and then derive a regional aerosol emission factor using the mean CO emission factor given by these authors, we obtain a value of $6.2 \text{ g kg}^{-1} \text{ dm}$. We conclude that a value of $4 \pm 1 \text{ g kg}^{-1} \text{ dm}$ appears to be a reasonable estimate for the mean aerosol emission factor from savanna and grassland fires, taking into account both airborne and ground-based measurements.

Particle Number and Volume Size Distributions

In Figure 8, we show the aerosol number size distributions in the plumes from 17 out of the 30 fires that we overflew (Table 1). To ensure representative data, only fires that offered relatively long and/or multiple passes through the plume are displayed. For this reason, the size distributions from fires like SAF08B-0, SAF08B-00, SAF12E, SAF14D, SAF14E, and SAF15G are not included. The graph shows that the shapes of the number distributions in the various plumes are very similar, although the individual aerosol emission rates varied greatly (Table 2). In the small size range, an exception is the plume from SAF06B (passes 14-22), where a shift of the distribution from smaller to bigger particles occurred because of hygroscopic growth in and near the cloud cap. The plume from SAF14A contains an unusually high fraction of particles in the $0.4\text{--}1.0 \mu\text{m}$ size range. No reason is evident for this anomalous behavior. In the smallest size range ($d < 0.2 \mu\text{m}$), the normalized $dN/d\log(d)$ values vary by less than a factor of 2 between fires. For the larger size particles ($d > 0.2 \mu\text{m}$), on the other hand, abundances vary considerably, up to a factor of 30.

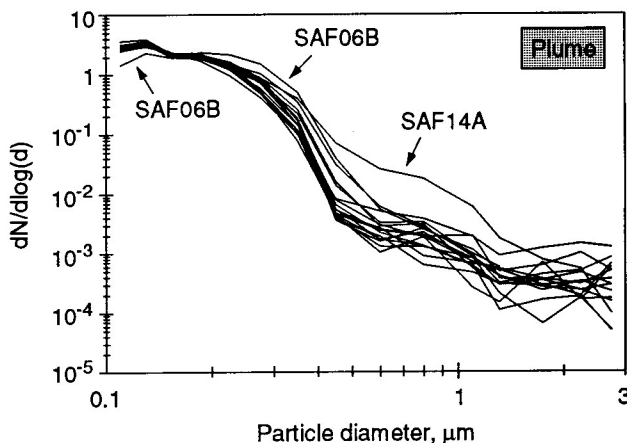


Figure 8. Normalized number size distribution in the plumes from 17 fires investigated during SAFARI-92.

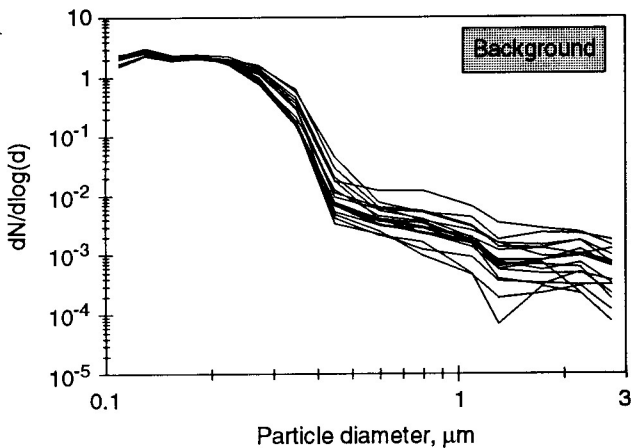


Figure 9. Normalized number size distribution in background air outside of the smoke plumes shown in Figure 8.

This is due to the very small absolute concentrations in the larger size range (about 10^6 times lower than in the small size range) which results in high variability. Typical aerosol number size distributions of the background aerosol are shown in Figure 9. The shapes of the background normalized number distributions are also very similar from one flight to the other. The same variability patterns found for the plumes also apply to the background.

There is a consistent difference between the aerosol number size distributions observed in the plume, in the background, and in the smoke (i.e., the plume after subtraction of the aerosol background). Since the normalization procedure removes the influence of the great difference in the absolute concentrations of particles in plumes and in the regional background, the average normalized number distributions can be compared directly (Figures 10a and 10b). On the same figure, we have plotted the averaged normalized size distribution of the smoke aerosol. We obtained this curve by subtracting the absolute size distribution of the background from that of the plume. The gap between $0.6 \mu\text{m}$ and $1 \mu\text{m}$ in the smoke particle size distribution is the result of higher average particle concentrations in the background than in the plume for this size range. The logarithmic scale emphasizes the variations in the large size range (Figure 10a), whereas the linear scale shows more clearly the differences in the small size range (Figure 10b). Furthermore, the linear representation in Figure 10b provides a direct impression of the amounts of particles present in each size range, since the area under the curve is directly proportional to the amount of particles present.

We observe a clear shift from a single maximum in the smallest two size classes ($0.10 < d < 0.14 \mu\text{m}$) in the smoke aerosol to somewhat larger average particle sizes and a secondary maximum at $0.2 \mu\text{m}$ in the background (Figures 10a and 10b). Since, in most cases, the background aerosol is dominated by aged smoke from biomass burning [Maenhaut et al., this issue; M. O. Andreae et al., manuscript in preparation, 1995; W. Maenhaut et al., manuscript in preparation, 1995], this trend may be due to particle growth and/or coagulation during aging. Number median diameters in fresh fire plumes are typically in the range $0.1 < d < 0.2 \mu\text{m}$ and evolve toward values in the range of $0.15 < d < 0.3 \mu\text{m}$ in the regional background aerosol. This is

in agreement with observations in the literature [Radke et al., 1991].

The normalized volume distributions ($dV/d\log(d)$) are shown for the smoke plumes in Figure 11 and for the regional background in Figure 12. Again, the shapes of the normalized distributions in the various plumes are very similar. Also, the two exceptions (SAF06B and SAF14A) seen previously in Figure 8 stand out clearly in Figure 11. The average normalized volume distributions for backgrounds, plumes and smoke particles are shown in Figures 13a and 13b. The background and plume distributions are similar, with three distinct modes at diameters of $0.2\text{--}0.4 \mu\text{m}$, near $1.0 \mu\text{m}$, and above $3.0 \mu\text{m}$. Unfortunately, the mode in the large size class is truncated by the upper end of the instrument's size range. The presence of a substantial aerosol mass fraction above the calibrated range of the instrument is suggested by the number of counts accumulated in the oversize bin of the counter. If one makes the conservative assumption that these particles have an average diameter of $3.5 \mu\text{m}$, i.e., one bin width greater than the largest calibrated size, the mass in this channel is enough to double or triple the observed mass in the supermicron range.

In the smallest mode of the volume size distribution, the same tendency toward larger particle size in the background compared to the smoke particles is evident as was observed in

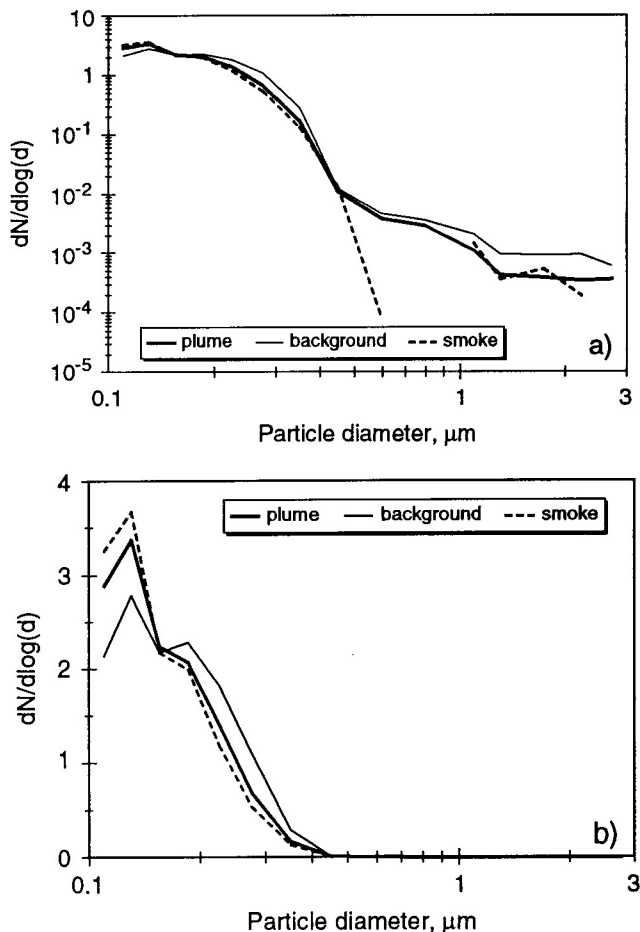


Figure 10. Average normalized number size distribution in the plumes and in background air outside of the smoke plumes shown on (a) a logarithmic and (b) a linear scale.

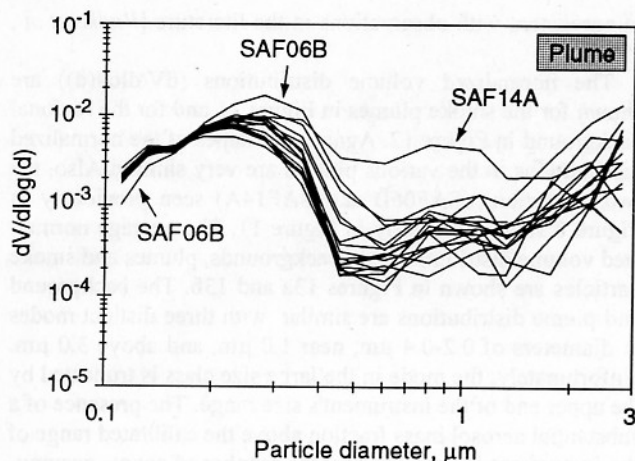


Figure 11. Normalized volume size distribution in the plumes from 17 fires investigated during SAFARI-92.

the number size distributions (Figures 10a and 10b). The size distributions in Figures 8-13 show that a significant fraction of the aerosol in the fire plumes is in the supermicron size range. The data suggest the presence of a coarse mode with a peak above $3 \mu\text{m}$, but the upper limit of the instrument's size range truncates this mode and does not allow an adequate characterization. In the pure smoke aerosol, i.e., after the background is subtracted from the plume aerosol, the coarse mode is still present, but considerably reduced in size. Observations made with filter packs and impactors also suggest that savanna fires release coarse aerosol particles which consist of soil dust and ash [Maenhaut *et al.*, this issue; M. O. Andreae, manuscript in preparation, 1995]. These observations are consistent with the measurements made in forest fire plumes by Radke *et al.* [1991], who found that the coarse mode represented an average of 20% of the mass of smoke emitted.

Conclusions

The SAFARI-92 experiment has provided us with estimates of aerosol emission ratios for savanna fires in several ecosystems in southern Africa. Our measurements in the fire plumes of experimental and agricultural fires show that the concentra-

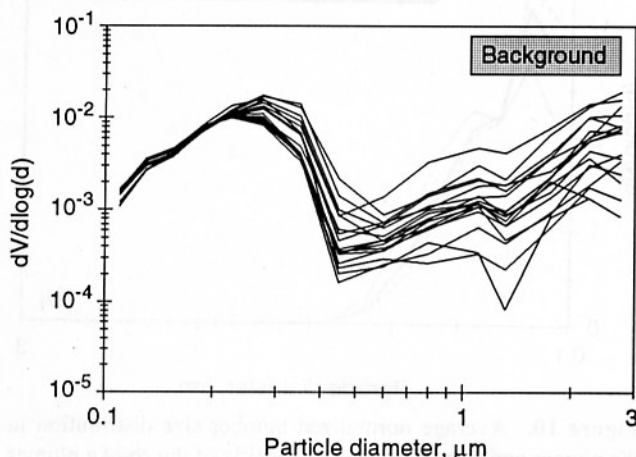


Figure 12. Normalized volume size distribution in background air outside of the smoke plumes shown in Figure 8.

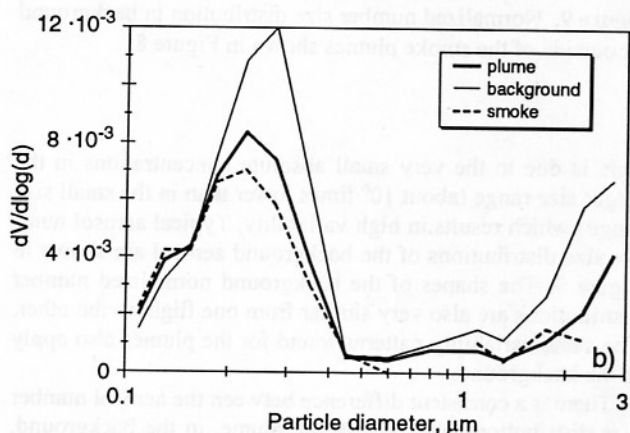
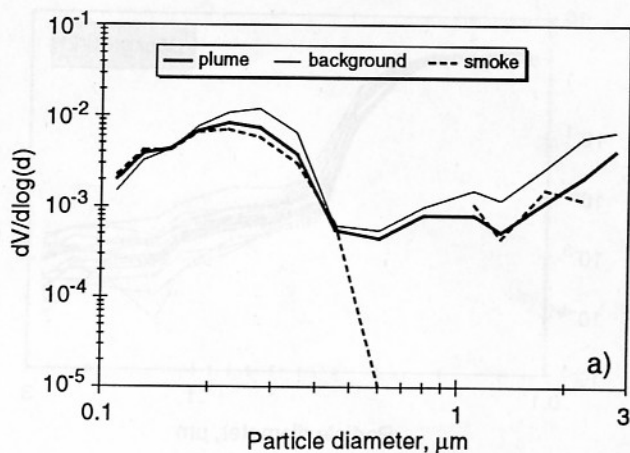


Figure 13. Average normalized volume size distribution in the plumes and in background air outside of the smoke plumes shown on (a) a logarithmic and (b) a linear scale.

tions of aerosol and CO are strongly correlated, making emission ratios based on the slope of the N versus CO regression a valuable tool for the regional and global estimation of aerosol emissions from savanna fires. We found significant differences between aerosol emission ratios from fires in different savanna ecosystems in the region. For the ecosystem classification, we used the vegetation fire regime map of the Division of Forest Science and Technology, Council for Scientific and Industrial Research, South Africa (R. S. Scholes, personal communication, 1994). Remote-sensing studies [Justice *et al.*, this issue; Scholes *et al.*, this issue] and our own observations show that most fires in the study region burn in moist, infertile savannas. We found savanna fires to have relatively low aerosol emission ratios: the average $\Delta\text{N}/\Delta\text{CO}$ is $23 \pm 7 \text{ cm}^{-3} \text{ ppb}^{-1}$ and $\Delta\text{M}/\Delta\text{CO}$ is $83 \pm 45 \text{ ng m}^{-3} \text{ ppb}^{-1}$ (Table 4). These fires are dominated by flaming combustion, as their CO-to-CO₂ emission ratio indicates ($\Delta\text{CO}/\Delta\text{CO}_2 = 0.048 \pm 0.025$). Infertile grasslands are the second ecosystem in which many fires are observed. The emission ratios from grassland fires are even lower, about half of those in the savannas: $\Delta\text{N}/\Delta\text{CO}$ is $14 \pm 2.3 \text{ cm}^{-3} \text{ ppb}^{-1}$ and $\Delta\text{M}/\Delta\text{CO}$ is $36 \pm 6.5 \text{ ng m}^{-3} \text{ ppb}^{-1}$ (Table 4). Fertile grasslands and savannas appeared to have somewhat higher emission ratios than their infertile counterparts, but the small data set from the fertile regions does not permit firm conclusions.

During SAFARI-92, which took place near the end of the dry season, fires in the seasonally flooded patches of grassland

called dambos were relatively infrequent. Fire scars in these areas suggested, however, that these grasslands had been burned over earlier in the season. These areas may be important sources of pyrogenic emissions, as the emission ratios from dambo fires were well above those from other types of fires. The particle number emission ratio relative to CO_2 was $2000 \pm 800 \text{ cm}^{-3} \text{ ppm}^{-1}$. High number and mass emission ratios were also observed from sugarcane fires: $\Delta N/\Delta \text{CO}$ was $43 \pm 4 \text{ cm}^{-3} \text{ ppb}^{-1}$ and $\Delta M/\Delta \text{CO}$ was $124 \pm 14 \text{ ng m}^{-3} \text{ ppb}^{-1}$ (Table 4). This type of fire is characterized by very rapid, flaming combustion, resulting in very low CO emission ratios ($\Delta \text{CO}/\Delta \text{CO}_2 = 0.03 \pm 0.01$).

On the basis of these emission ratios, we estimated the corresponding aerosol mass emission factors, which varied between 1.3 and $8.3 \text{ g kg}^{-1} \text{ dm}$. The average emission factor for savannas and grasslands, weighted by the amount of carbon burned in the various ecosystems, is $3.6 \text{ g kg}^{-1} \text{ dm}$. These results compare satisfactorily with the ground-based, gravimetric determinations of aerosol emission factors made during SAFARI-92, which yielded a weighted mean of $4.8 \text{ g kg}^{-1} \text{ dm}$ for savanna and grassland fires [Scholes *et al.*, this issue]. The emission factors from the savanna fires studied during SAFARI-92 ($1.3\text{--}8.3 \text{ g kg}^{-1} \text{ dm}$) agree with literature estimates for flaming fires ($2\text{--}10 \text{ g kg}^{-1} \text{ dm}$ [Radke *et al.*, 1991; Andreae, 1993a, and references therein]).

The distribution of the number and mass emission ratios as a function of the CO-to- CO_2 emission ratio (Figure 6) suggests that the most intensely flaming fires have higher emission ratios relative to CO than the more common fires that have CO-to- CO_2 emission ratios around 6%. No clear relationship between aerosol emission factors and combustion efficiencies was evident in our data, in contrast to previous studies [Ward *et al.*, 1992, this issue].

Although the different emission ratios varied widely from one ecosystem to the other, the particle number and volume distributions as a function of particle size were very similar for most of the plumes. This also applies to the size distribution of the background aerosol and the pure smoke aerosol (i.e., the size distribution in the smoke plumes corrected for the background distribution). On the basis of our measurements, we can therefore define average number and volume distributions characteristic of fresh smoke from savanna fires. Two modes are evident in the average smoke volume size distribution, the first centered on $0.2\text{--}0.3 \mu\text{m}$ and the second in the size range $>2 \mu\text{m}$.

Finally, we can estimate the annual emission of aerosols from savanna burning worldwide, using an estimate of $3690 \text{ Tg dm yr}^{-1}$ for the yearly amount of biomass burned in savanna ecosystems [Andreae, 1993a]. With the estimated range for the regional mean emission factor from fires in the various savanna ecosystems ($4 \pm 1 \text{ g kg}^{-1} \text{ dm}$), we obtain a range of $11\text{--}18 \text{ Tg yr}^{-1}$ for the global annual emission of particles $<3 \mu\text{m}$ from savanna fires. For comparison, the annual emission of aerosols from the burning of tropical forests is estimated to be 19 Tg yr^{-1} , based on a mean emission factor of $15 \text{ g kg}^{-1} \text{ dm}$ and a total biomass burned of $1260 \text{ Tg dm yr}^{-1}$ [Andreae, 1993a]. Although the amount of biomass burned in savannas is 3 times as large as that burned in tropical forests, the resulting annual emission of fine particles is probably less. Thus savanna fires are not as prominent sources of pyrogenic aerosol as might have been expected from the large amount of biomass burned in these ecosystems each year. Nevertheless, these fires ac-

count for some 10-20% of the pyrogenic aerosols released globally.

The number of cloud condensation nuclei (CCN) released from savanna fires can be estimated using either the CO- or the CO_2 -based emission ratios. With a range of $\Delta N/\Delta \text{CO}$ of $20\text{--}40 \text{ cm}^{-3} \text{ ppb}^{-1}$ and a global emission of $100 \text{ Tg C(CO) yr}^{-1}$ from savanna fires, we obtain a particle emission rate of $4\text{--}8 \times 10^{27} \text{ yr}^{-1}$; using a range of $\Delta N/\Delta \text{CO}_2$ of $1000\text{--}2000 \text{ cm}^{-3} \text{ ppm}^{-1}$ and a value of $3690 \text{ Tg dm yr}^{-1}$ for the yearly amount of biomass burned in savannas, the particle emission rate is $3\text{--}6 \times 10^{27} \text{ yr}^{-1}$. Given that, on one hand, our measurements are limited to the size range above $0.1 \mu\text{m}$, whereas the range of potential CCN extends to somewhat lower diameters, and that on the other hand, some 30-100% of submicron biomass smoke particles can act as CCN [Rodgers *et al.*, 1991], our estimate of particle emission is probably also a reasonable estimate of the CCN production from savanna fires. This value can be compared to Radke *et al.*'s [1991] estimate of pyrogenic CCN production, $35 \times 10^{27} \text{ yr}^{-1}$. These authors state that a production rate of this magnitude is comparable to estimates of CCN production from marine and industrial sources. By measurements in smoke layers over the western South Atlantic, which had originated in Africa, we were able to show that pyrogenic aerosols can be transported over subhemispheric distances without substantial removal [Andreae *et al.*, 1994a]. Given the geographically and seasonally focused range of smoke emission from savanna fires, our results suggest that they exert a dominant influence on the number and composition of aerosols present in the dry and subhumid tropics during the dry part of the year [Le Canut *et al.*, 1996; M. O. Andreae *et al.*, manuscript in preparation, 1995] and that the influence of pyrogenic CCN may well extend to the free troposphere over large parts of the tropical oceans.

Acknowledgments. We thank the pilots and crews of the SAFARI-92 DC-3 research aircraft for their assistance during the research flights, the Kruger Park team (particularly A. Potgieter, W. Trollope, L. Trollope, and J. G. Goldammer) for their untiring cooperation during the experimental fires in the park, and the team at the sugar plantation at Ubombo Ranches, Big Bend, Swaziland (especially J. Gosnell and D. Shipley) for their generous help during our experiment. We acknowledge the permission of various government agencies in Angola, Botswana, South Africa, Namibia, Swaziland, Zambia, and Zimbabwe for permission to conduct research in these countries or to use the airspace over these countries. We appreciate the help of T. W. Andreae (logistical support) and U. Parchatka (technical support) during the airborne sampling missions on the DC-3 aircraft. Partial support of DC-3 aircraft program by the National Science Foundation is gratefully acknowledged. This research was supported by the Max Planck Society. Correspondence regarding this paper should be addressed to M. O. A.

References

- Andreae, M. O., The influence of tropical biomass burning on climate and the atmospheric environment, in *Biogeochemistry of Global Change: Radiatively Active Trace Gases*, edited by R. S. Oremland, pp. 113-150, Chapman and Hall, New York, 1993a.
- Andreae, M. O., Global distribution of fires seen from space, *Eos Trans. AGU*, **74**, 129-135, 1993b.
- Andreae, M. O., Climatic effects of changing atmospheric aerosol

- levels, in *World Survey of Climatology, Vol. 16: Future Climates of the World*, edited by A. Henderson-Sellers, pp. 341-392, Elsevier, Amsterdam, 1995.
- Andreae, M. O., et al., Biomass-burning emissions and associated haze layers over Amazonia, *J. Geophys. Res.*, **93**, 1509-1527, 1988.
- Andreae, M. O., B. E. Anderson, D. R. Blake, J. D. Bradshaw, J. E. Collins, G. L. Gregory, G. W. Sachse, and M. C. Shipman, Influence of plumes from biomass burning on atmospheric chemistry over the equatorial and tropical South Atlantic during CITE-3, *J. Geophys. Res.*, **99**, 12,793-12,808, 1994a.
- Andreae, M. O., J. Fishman, M. Garstang, J. G. Goldammer, C. O. Justice, J. S. Levine, R. J. Scholes, B. J. Stocks, A. M. Thompson, B. van Wilgen, and the STARE/TRACE-A/SAFARI Science Team, Biomass burning in the global environment: First results from the IGAC/BIBEX field campaign STARE/TRACE-A/SAFARI-92, in *Global Atmospheric-Biospheric Chemistry*, edited by R. G. Prinn, pp. 83-101, Plenum, New-York, 1994b.
- Andreae, M. O., E. Atlas, H. Cachier, W. R. Cofer III, G. W. Harris, G. Helas, R. Koppmann, J. P. Lacaux, and D. E. Ward, Trace gas and aerosol emissions from savanna fires, in *Biomass Burning and Global Change*, edited by J. S. Levine, MIT Press, Cambridge, Mass., in press, 1996.
- Cahoon, D. R., Jr., B. J. Stocks, J. S. Levine, W. R. Cofer, III, and K. P. O'Neill, Seasonal distribution of African savanna fires, *Nature*, **359**, 812-815, 1992.
- Charlson, R. J., S. E. Schwartz, J. M. Hales, R. D. Cess, J. A. Coakley, Jr., J. E. Hansen, and D. J. Hofmann, Climate forcing by anthropogenic aerosols, *Science*, **255**, 423-430, 1992.
- Cofer, W. R., III, J. S. Levine, E. L. Winstead, D. R. Cahoon, D. I. Sebacher, J. P. Pinto, and B. J. Stocks, Source composition of trace gases released during African savanna fires, *J. Geophys. Res.*, this issue.
- Crutzen, P. J., and M. O. Andreae, Biomass burning in the tropics: Impact on atmospheric chemistry and biogeochemical cycles, *Science*, **250**, 1669-1678, 1990.
- Dickinson, R. E., Effect of fires on global radiation budget through aerosol and cloud properties, in *Fire in the Environment: The Ecological, Atmospheric, and Climatic Importance of Vegetation Fires*, edited by P. J. Crutzen and J. G. Goldammer, pp. 107-122, John Wiley, New York, 1993.
- Einfeld, W., D. E. Ward, and C. Hardy, Effects of fire behavior on prescribed fire smoke characteristics: A case study, in *Global Biomass Burning: Atmospheric, Climatic, and Biospheric Implications*, edited by J. S. Levine, pp. 412 - 419, MIT Press, Cambridge, Mass., 1991.
- Garstang, M., P. D. Tyson, R. Swap, M. Edwards, P. Källberg, and J. A. Lindsay, Horizontal and vertical transport of air over southern Africa, *J. Geophys. Res.*, this issue.
- Harris, G. W., T. Zenker, F. G. Wienhold, M. Welling, U. Parchatka, and M. O. Andreae, Airborne measurements of trace gas emission ratios from southern African veld fires (abstract), *Eos Trans. AGU*, **74** (43), Fall Meet. Suppl., 104, 1993.
- Helas G., J. Lobert, D. Scharffe, L. Schäfer, J. Goldammer, J. Baudet, A. Ajavon, A. Brou, J. P. Lacaux, R. Delmas, and M. O. Andreae, Airborne measurements of vegetation burning products over western Africa, *J. Atmos. Chem.*, **22**, 217-239, 1995.
- Jones, A., D. L. Roberts, and A. Slingo, A climate model study of indirect radiative forcing by anthropogenic sulphate aerosols, *Nature*, **370**, 450-453, 1994.
- Justice, C. O., J. D. Kendall, P. R. Dowty, and R. J. Scholes, Satellite remote sensing of fires during the SAFARI campaign using NOAA-AVHRR data, *J. Geophys. Res.*, 1996, this issue.
- Koppmann, R., A. Khedim, J. Rudolph, G. Helas, M. Welling, and T. Zenker, Airborne measurements of organic trace gases from savanna fires in southern Africa, in *Biomass Burning and Global Change*, edited by J. S. Levine, MIT Press, Cambridge, Mass., in press, 1996.
- Lacaux, J. P., R. Delmas, C. Jambert, and T. Kuhlbusch, NO_x emissions from African savanna burning, *J. Geophys. Res.*, 1996, this issue.
- Lacaux, J. P., J. M. Brustet, R. Delmas, J. C. Menaut, L. Abbadie, B. Bonsang, H. Cachier, J. Baudet, M. O. Andreae, and G. Helas, Biomass burning in the tropical savannas of Ivory Coast: An overview of the field experiment Fire Of Savannas (FOS/DECAFE '91), *J. Atmos. Chem.*, **22**, 195-216, 1995.
- Le Canut, P., M. O. Andreae, G. W. Harris, F. G. Wienhold, and T. Zenker, Aerosol optical properties over southern Africa during SAFARI-92, in *Biomass Burning and Global Change*, edited by J. S. Levine, MIT Press, Cambridge, Mass., in press, 1996.
- Maenhaut, W., I. Salma, J. Cafmeyer, H. J. Annegarn, and M. O. Andreae, Regional atmospheric aerosol composition and sources in the eastern Transvaal, South Africa, and impact of biomass burning, *J. Geophys. Res.*, this issue.
- Radke, L. F., D. A. Hegg, P. V. Hobbs, J. D. Nance, J. H. Lyons, K. K. Laursen, R. E. Weiss, P. J. Riggan, and D. E. Ward, Particulates and trace gas emissions from large biomass fires in North America, 209-224, in *Global Biomass Burning: Atmospheric, Climatic, and Biospheric Implications*, edited by J. S. Levine, pp. 209-224, MIT Press, Cambridge, Mass., 1991.
- Rodgers, C. F., J. G. Hudson, B. Zielinska, R. L. Tanner, J. Hallett, and J. G. Watson, Cloud condensation nuclei from biomass burning, in *Global Biomass Burning: Atmospheric, Climatic, and Biospheric Implications*, edited by J. S. Levine, pp. 431-438, MIT Press, Cambridge, Mass., 1991.
- Scholes, R. J., D. Ward, and C. O. Justice, Emissions of trace gases and aerosol particles due to vegetation burning in southern hemisphere Africa, *J. Geophys. Res.*, this issue.
- Stocks, B. J., B. W. van Wilgen, W. S. W. Trollope, D. J. McRae, J. A. Mason, F. Weirich, and A. L. F. Potgieter, Fuels and fire behavior on large-scale savanna fires in Kruger National Park, South Africa, *J. Geophys. Res.*, this issue.
- Swap, R., M. Garstang, S. A. Macko, P. D. Tyson, W. Maenhaut, P. Artaxo, P. Källberg, and R. Talbot, The long-range transport of southern African aerosols to the tropical South Atlantic, *J. Geophys. Res.*, this issue.
- Ward, D. E., and C. C. Hardy, Smoke emissions from wildland fires, *Environ. Int.*, **17**, 117-134, 1991.
- Ward, D. E., A. W. Setzer, Y. J. Kaufman, and R. A. Rasmussen, Characteristics of smoke emissions from biomass fires of the Amazon region - BASE-A experiment, in *Global Biomass Burning: Atmospheric, Climatic, and Biospheric Implications*, edited by J. S. Levine, pp. 394-402, MIT Press, Cambridge, Mass., 1991.
- Ward, D. E., R. A. Susott, J. B. Kauffman, R. E. Babbitt, D. L. Cummings, B. Dias, B. N. Holben, Y. J. Kaufman, R. A. Rasmussen, and A. W. Setzer, Smoke and fire characteristics for cerrado and deforestation burns in Brazil: BASE-B Experiment, *J. Geophys. Res.*, **97**, 14,601-14,619, 1992.
- Ward, D. E., W.-M. Hao, R. A. Susott, R. A. Babbitt, R. W. Shea, J. B. Kauffman, and C. O. Justice, Effect of fuel composition on combustion efficiency and emission factors for African savanna ecosystems, *J. Geophys. Res.*, this issue.
- Wienhold, F. G., T. Zenker, and G. W. Harris, A dual channel two tone frequency modulation tunable diode laser spectrometer for ground-based and airborne trace gas measurements, paper presented at the International Symposium on Optical Sensing for Environmental Monitoring, Atlanta, Ga., Oct. 11-15, 1993.

M. O. Andreae and P. Le Canut, Biogeochemistry Department, Max Planck Institute for Chemistry, P. O. Box 3060, D-55020 Mainz, Germany (e-mail: moa@mpch-mainz.mpg.de)

G. W. Harris, Centre for Atmospheric Chemistry, York University, North York, Ontario, Canada M3J 1P3, Canada.

F. G. Wienhold and T. Zenker, Air Chemistry Department, Max Planck Institute for Chemistry, P. O. Box 3060, D-55020 Mainz, Germany.

(Received January 31, 1995; revised July 14, 1995; accepted July 31, 1995.)